

## SPECTRAL TYPES FOR FOUR OGLE-III TRANSIT CANDIDATES: COULD THESE BE PLANETS?

A. N. HEINZE AND PHILIP M. HINZ

Steward Observatory, University of Arizona, 933 North Cherry Avenue, Tucson, AZ 85721-0065;  
aheinze@as.arizona.edu, phinz@as.arizona.edu

Received 2005 February 21; accepted 2005 June 15

### ABSTRACT

We present spectral types for OGLE (Optical Gravitational Lensing Experiment) transiting planet candidates OGLE-TR-134 through 137 based on low-resolution spectra taken at Kitt Peak. Our main objective is to aid those planning radial velocity monitoring of transit candidates. We obtain spectral types with an accuracy of 2 spectral subtypes, along with tentative luminosity classifications. Combining the spectral types with light-curve fits to the OGLE transit photometry, and with Two Micron All Sky Survey counterparts in two cases, we conclude that OGLE-TR-135 and 137 are not planetary transits, while OGLE-TR-134 and 136 are good candidates and should be observed with precision radial velocity monitoring to determine whether the companions are of planetary mass. OGLE-TR-135 is ruled out chiefly because a discrepancy between the stellar parameters obtained from the transit fit and those inferred from the spectra indicates that the system is a blend. OGLE-TR-137 is ruled out because the depth of the transit combined with the spectral type of the star indicates that the transiting object is stellar. OGLE-TR-134 and 136, if unblended main-sequence stars, are each orbited by a transiting object with radius below  $1.4 R_J$ . The caveats are that our luminosity classification suggests that OGLE-TR-134 could be a giant (and therefore a blend), while OGLE-TR-136 shows a (much smaller) discrepancy of the same form as OGLE-TR-135, which may indicate that the system is a blend. However, since our luminosity classifications are uncertain at best, and the OGLE-TR-136 discrepancy can be explained if the primary is a slightly anomalous main-sequence star, the stars remain good candidates.

*Key words:* binaries: eclipsing — planetary systems — stars: individual (OGLE-TR-134, OGLE-TR-135, OGLE-TR-136, OGLE-TR-137) — techniques: spectroscopic

### 1. INTRODUCTION

OGLE (Optical Gravitational Lensing Experiment) has proved the most successful project to date at finding extrasolar planets by their photometric transits. Such discoveries remain difficult, however: of the first 137 OGLE transit candidates released (Udalski et al. 2002a, 2002b, 2002c, 2003), only four have been confirmed and published as true planets to date (Konacki et al. 2003; Pont et al. 2004; Bouchy et al. 2004). Most of the rest are stellar eclipsing binaries that show a shallow, transit-like light curve, frequently because the eclipsing binary is in an unresolved blend with a brighter star that dilutes the eclipse depth or because the size ratio of the stars is very high and the eclipses are thus very shallow (Dreizler et al. 2002; Konacki et al. 2003).

The only way to confirm a planetary transit candidate in a final sense is to make precise radial velocity observations of the star and detect a planetary radial velocity signature that exhibits the same period and phase as the planetary orbit inferred from the transit. For faint stars such as the OGLE transits ( $I \sim 15$ ), radial velocity determination of sufficient precision requires a 6–10 m telescope, and, of course, several measurements must be made to sample the orbit sufficiently. These requirements make radial velocity observations of the entire list of OGLE candidates very telescope-intensive, so a preliminary screening to identify the candidates most likely to harbor true planets is desirable.

Spectroscopy to determine spectral types is a good method for such screening. It can be done on a much smaller telescope and can easily rule out many candidates. In many cases a candidate will be ruled out because when the theoretical radius for a star of the measured spectral type is combined with the measured transit depth to deduce the transiting object's true radius, the result indicates that the object is too big to be a planet and is thus a low-mass star (Dreizler et al. 2002). In other cases spectroscopy may indicate that

the star is a giant. This means that the system is most likely a blend, with the “transit” signal coming from a faint eclipsing binary and the majority of the light coming from an unrelated giant star in an unresolved blend with the binary. In yet other cases the results from spectroscopy may indicate a radius and mass for the star that is far different from the radius and mass that can be derived from a fit to the transit light curve. Depending on the form and severity of this discrepancy it may be sufficient to conclude that the system is a blend or that the primary is an anomalous star with a radius too large for the observed transit to be caused by a planet.

Advances in radial velocity follow-up strategy and OGLE candidate selection may make it possible to follow up all or most of the OGLE candidates (Bouchy et al. 2004), thus rendering a preliminary screening unnecessary. However, low-resolution spectroscopic observations still have value, because they allow a spectral classification of the stars that is effectively independent of the classification that can be obtained from the radial velocity spectra, which have much higher resolution but not the same spectral range.

We present spectral types for OGLE transit candidates OGLE-TR-134 through 137 based on low-resolution spectra. We choose these stars because they are the last stars from the 2001 OGLE-III observing campaign that have not yet been included in a low-resolution spectroscopic screening program, as the other 2001 OGLE-III transit candidates were in Dreizler et al. (2002) and Konacki et al. (2003). Our four candidates were not analyzed in these earlier papers because they were identified only on re-analysis of the 2001 data with an improved algorithm to remove systematic error (Udalski et al. 2003, hereafter U03). They had evaded detection in the earlier analysis (Udalski et al. 2002c) because the transits were very shallow; thus, this is a sample that is particularly likely to contain objects small enough to be true planets. This work, combined with Dreizler et al. (2002) and Konacki et al. (2003), completes the preliminary screening of all

of the 2001 OGLE-III planetary transit candidates. The screening is complete in the sense that every 2001 OGLE-III transit candidate for which good spectra could be taken and for which transit photometry was broadly consistent with a planetary interpretation has been examined by low-resolution spectroscopy; in some cases the star was too faint or confused to be a practical target, or the OGLE-III photometry recorded only a single transit or showed clear evidence of a stellar companion (Dreizler et al. 2002; Konacki et al. 2003; Sirko & Paczynski 2003). Gallardo et al. (2005) have screened the 2002 OGLE-III transit candidates published in Udalski et al. (2002b) in the same way. U03 present new candidates identified in reanalysis of the 2002 data in addition to the 2001 candidates we analyze here, but we were not able to include any of the 2002 objects in our program because all of them lie too far south to be observed from Kitt Peak.

We describe the observations and data reduction in § 2 and the classification methods and results in § 3. In § 4 we discuss the implications of our results and compare them to other work. In § 5 we present our conclusions, and in § 6 we make recommendations for future work.

## 2. OBSERVATIONS AND DATA REDUCTION

On the nights of 2004 June 12 and 13, we used the Boller & Chivens spectrograph on the University of Arizona's 2.3 m Bok Telescope at Kitt Peak to obtain low-resolution spectra of OGLE-TR-134 through 137. We used a 600 grooves  $\text{mm}^{-1}$  grating blazed to 4458 Å, yielding a sampling of about  $1.86 \text{ Å pixel}^{-1}$ , a resolution of about 5 Å, and spectral coverage from 3800 to 6000 Å. Because the science targets were all near  $-30^\circ$  declination and at similar right ascension, they were only observable for about 4 hr each night. During the remainder of each night we observed bright stars of spectral types and luminosity classes ranging from type A to M and class V to I. We did this to provide a set of spectra of well-known type taken under the same conditions as our science targets to aid in the classification of our targets. These were found to be very useful in ascertaining the accuracy of our classifications, as is seen below. Both nights were mostly or completely clear, and no effect from clouds was noticed during the observations of our science targets. See Table 1 for details of the observations.

In our data reduction we used IRAF to subtract a bias frame from the images and correct for constant bad columns and bad pixels and then used the *lacos\_spec* program (van Dokkum 2001)<sup>1</sup> to remove cosmic rays, of which there were many. The rest of the data analysis was carried out using custom code written by one of us (A. H.), which was superior to IRAF only in that it was more transparent and easier to tweak. This software performed flat-fielding (using flats normalized for each wavelength to preserve the detected photon fluence and ease statistical analysis), spectrum tracing and extraction, sky subtraction, wavelength calibration and resampling, continuum normalization, and blurring to match the resolution of the spectrum catalogs we used for classification. The blurring was a convolution with a Gaussian of  $\sigma = 3.5 \text{ Å}$ , and this proved very important to allow precise comparison of our spectra with those in the catalogs. The final products of our data analysis were spectra with 5 Å sampling spanning the wavelength range from 3800 to 6000 Å, with the continuum normalized to 1.0.

## 3. CLASSIFICATION

We determined the spectral types of our stars using two independent methods, one manual and one automated, and two dif-

TABLE 1  
OBSERVATIONS OF THE SCIENCE TARGETS

Star	<i>I</i> (mag)	Integration Time (s)	S/N Range
OGLE-TR-134 .....	13.49	2400	26–56
OGLE-TR-135 .....	15.16	6600	19–33
OGLE-TR-136 .....	14.93	6600	19–34
OGLE-TR-137 .....	15.85	7800	31–40

NOTES.—Magnitudes are from U03. The total integration time was broken up into exposures of 600 s each to avoid excessive cosmic-ray hits. “S/N range” refers to the S/N per pixel on the final summed spectra from the shortest to longest wavelengths we used in classification, i.e., from Ca II H and K near 3800 Å to H $\beta$  near 4800 Å.

ferent atlases of standard spectra, that from Pickles (1998) and from Silva & Cornell (1992).<sup>2</sup> In our manual classification, which we performed first, we visually compared resolution-matched and continuum-normalized versions of our spectra with the atlas spectra from Pickles (1998). We used Abt et al. (1968) as a guide for what to look for. We classified seven stars of known spectral type ranging from A to K and the four science targets. We arranged the classification carefully so that the classifier could have no knowledge of what star he was classifying or whether it was a science target or a standard. The classification was thus as unbiased as possible by prior knowledge of or conclusions about the spectral types. See Figures 1–4 for examples of the spectra and graphical demonstrations of the classifications.

Based on Abt et al. (1968) and our experience with manual spectral classification, we identified seven spectral regions useful for classifying stars of spectral types A5–K5. Each region contains a prominent line or set of lines (see Table 2).

We produced a code to perform automated spectral classification by least-squares matching of our spectra to the atlas spectra within the useful regions we had identified. For the atlas we used spectra from both the Silva & Cornell (1992) and the Pickles (1998) catalogs. The weight given to each spectral region in the classification was inversely proportional to the mean rms variation across all the stars in the atlas within that region; thus, deviations in the region of the Ca II H and K lines, which varied enormously across the atlas, were weighted less than deviations in the vicinity of the 4172–4179 Å blend, which changed much more subtly with spectral type and luminosity class. To determine the final classification a number was assigned to each spectral subtype, ranging from 0.0 (type A0) to 37.0 (type K7), and another to each luminosity class, ranging from 1.0 (class I) to 5.0 (class V). This defined a two-dimensional space in which all normal stars in the specified range of spectral types could be located. The automated classification algorithm found the three atlas points with the lowest weighted rms deviation from the input spectrum and then did an error-weighted average of these three best points to determine the final classification. This was found to be quite effective for determining the true spectral type, provided the star to be classified did not lie too near the endpoints A0 and K7 (a condition met by all our science targets). The algorithm ran into difficulties for determining luminosity class, because the extreme values, 1.0 for a supergiant or 5.0 for a dwarf, were not correctly obtained unless all three best matches had the same luminosity class. The atlases did not fill the two-dimensional spectral classification space sufficiently well to make this a likely outcome, so most dwarfs were classified as

<sup>1</sup> This software is available for download at <http://www.astro.yale.edu/dokkum/lacosmic>.

<sup>2</sup> Both of these atlases can be found at <http://www.phys.unm.edu/~cpo/html/twhtml/spectra/spectra.html>.

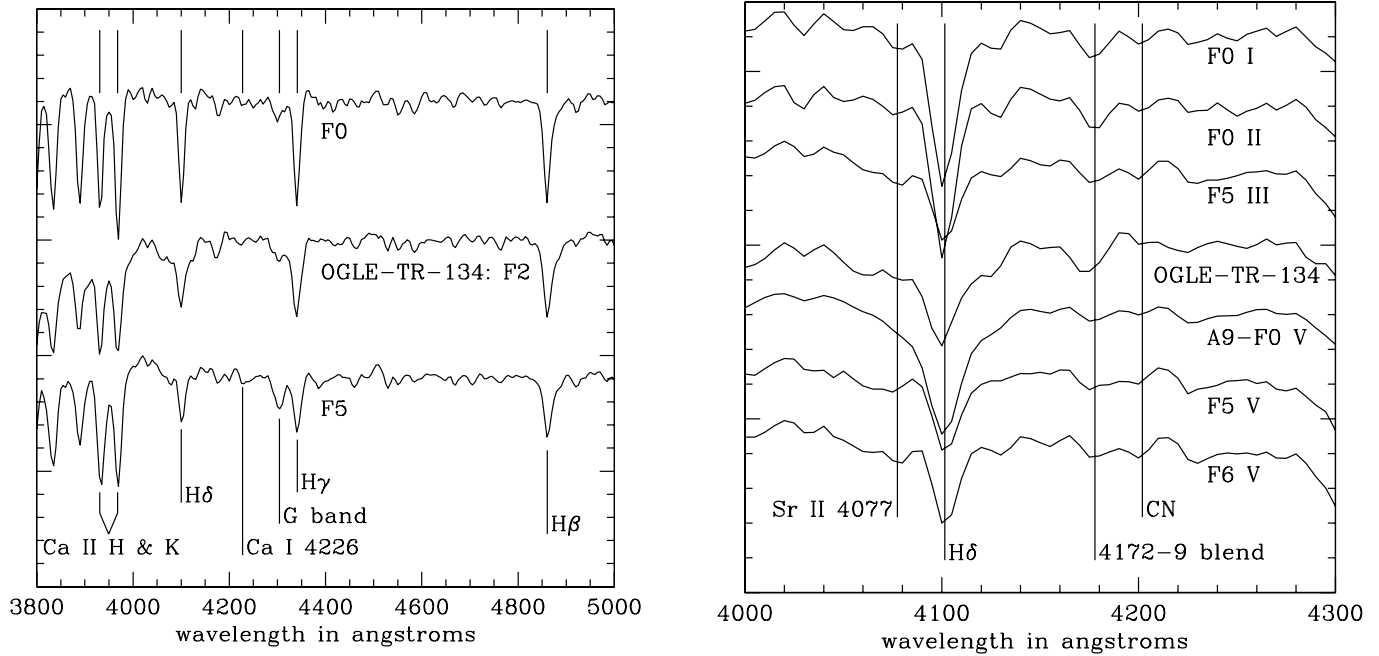


FIG. 1.—Classification of OGLE-TR-134: F2, probable giant. The spectral typing is demonstrated on the left and the luminosity classification on the right. The key lines for spectral typing in this regime are the Balmer H lines and the G band, with the intensity of the Balmer lines decreasing and that of the G band increasing toward later spectral types. The most useful line for luminosity classification is the blend at 4172–4179 Å, which is stronger in giant stars than in dwarfs. As is clear, spectral type is determined much more confidently than luminosity class. All the comparison spectra are taken from the Pickles (1998) atlas, except the A9–F0 V spectrum, which is from Silva & Cornell (1992).

slightly less than 5.0 and most supergiants slightly above 1.0. This bias away from the extreme luminosity classifications must be taken into account when interpreting the automated classification results.

We used our automated code to classify the seven known stars that had been classified manually, six other known stars that had

not been classified manually, and the four science targets. See Table 3 for the classification results.

The data in Table 3 give an indication of the accuracy of both methods of classification. For the seven known stars classified with both methods, the manual classification has an rms error of 1.58 spectral subtypes and 0.58 luminosity classes, while the

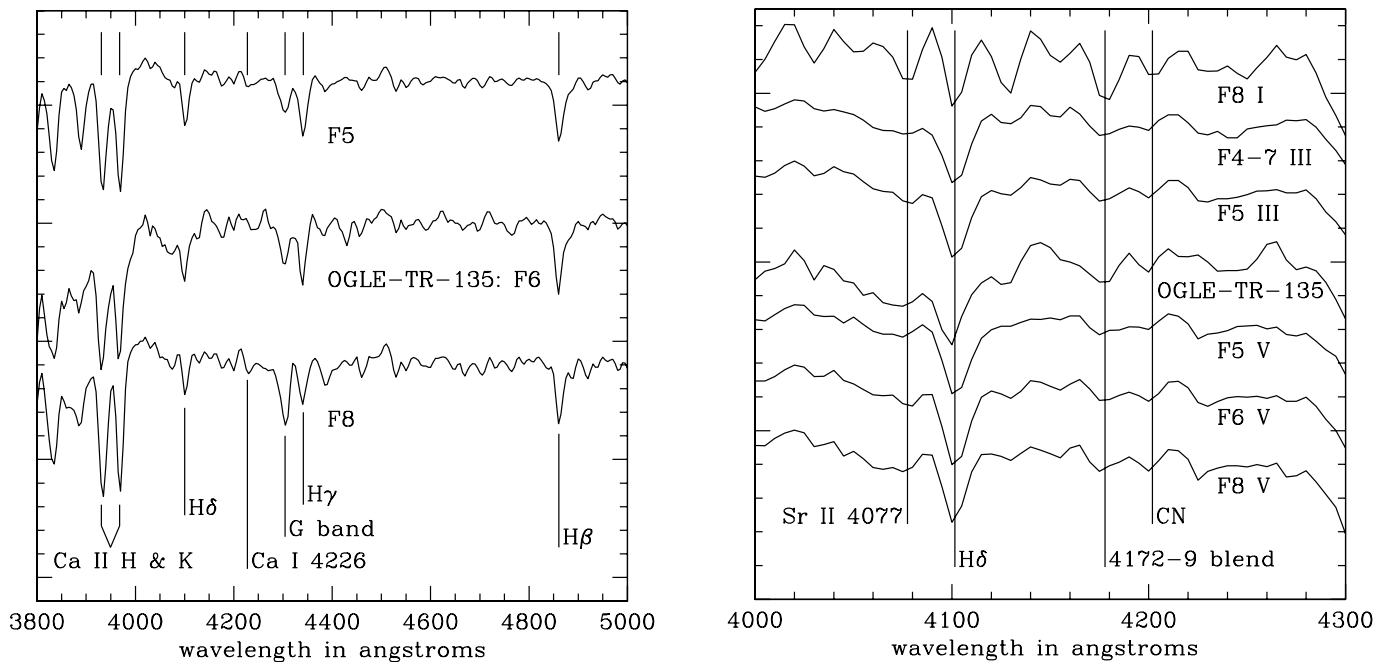


FIG. 2.—Classification of OGLE-TR-135: F6, probable giant. The spectral typing is demonstrated on the left and the luminosity classification on the right. The key lines for spectral typing in this regime are the Balmer H lines and the G band, with the intensity of the Balmer lines decreasing and that of the G band increasing toward later spectral types. The lines useful for luminosity classifications are the blend at 4172–4179 Å, the CN feature near 4203 Å, and Sr II  $\lambda$ 4077, which are all stronger in giant stars than in dwarfs. As is clear, spectral type is determined much more confidently than luminosity class. All the comparison spectra are taken from the Pickles (1998) atlas, except the F4–7 III spectrum, which is from Silva & Cornell (1992).

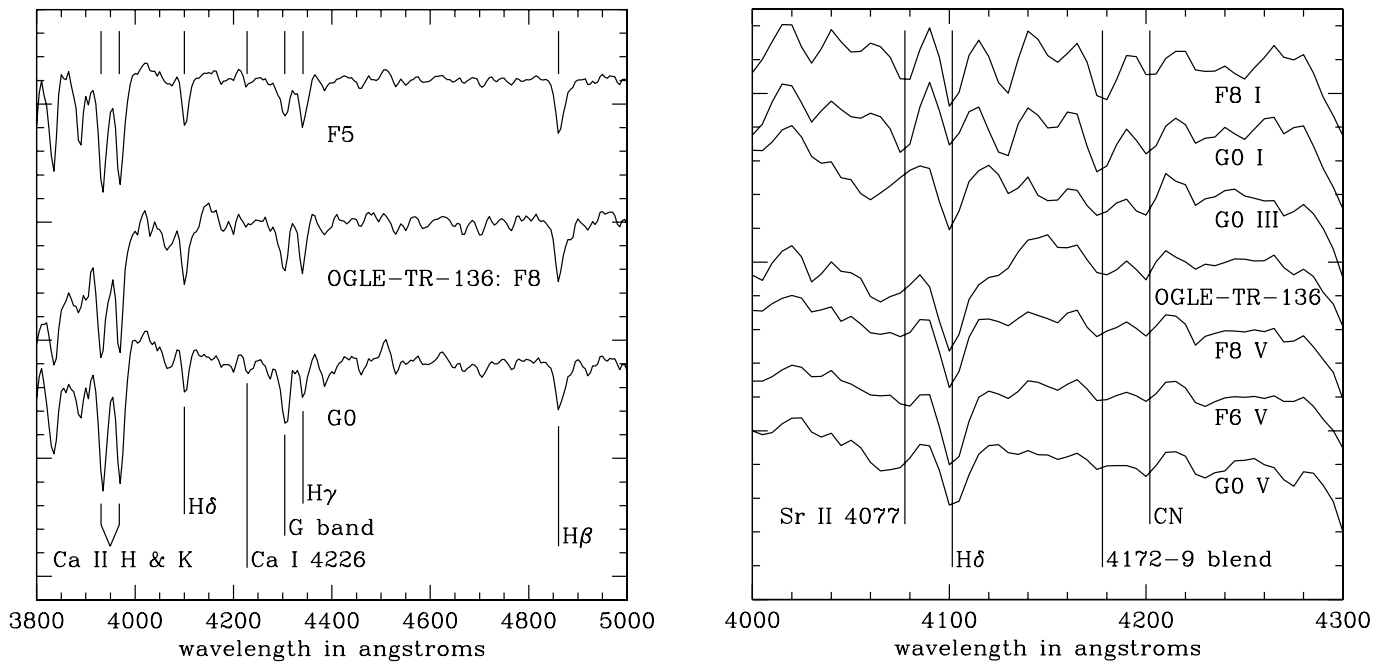


FIG. 3.—Classification of OGLE-TR-136: F8, probable dwarf. The spectral typing is demonstrated on the left and the luminosity classification on the right. The key lines for spectral typing in this regime are the Balmer H lines and the G band, with the intensity of the Balmer lines decreasing and that of the G band increasing toward later spectral types. The lines useful for luminosity classifications are the blend at 4172–4179 Å, the CN feature near 4203 Å, and Sr II  $\lambda$ 4077, which are all stronger in giant stars than in dwarfs. As is clear, spectral type is determined much more confidently than luminosity class. All the comparison spectra are taken from Pickles (1998).

automated classification has an rms error of 1.40 spectral subtypes and 0.96 luminosity classes. For these seven stars, the rms difference between the manual and computer classifications is 2.34 spectral subtypes and 1.07 luminosity classes. For the whole list of 13 known stars classified by the automated method, the automated method has an rms error of 1.34 spectral subtypes

and 1.2 luminosity classes. The rms difference between the manual and automated classifications of the science targets is 2.46 spectral subtypes and 1.10 luminosity classes.

These statistics, combined with the details in Table 3, make it clear that the spectral typing is quite good, with a true  $1\sigma$  error of less than 2 subtypes, while the luminosity classification is rather

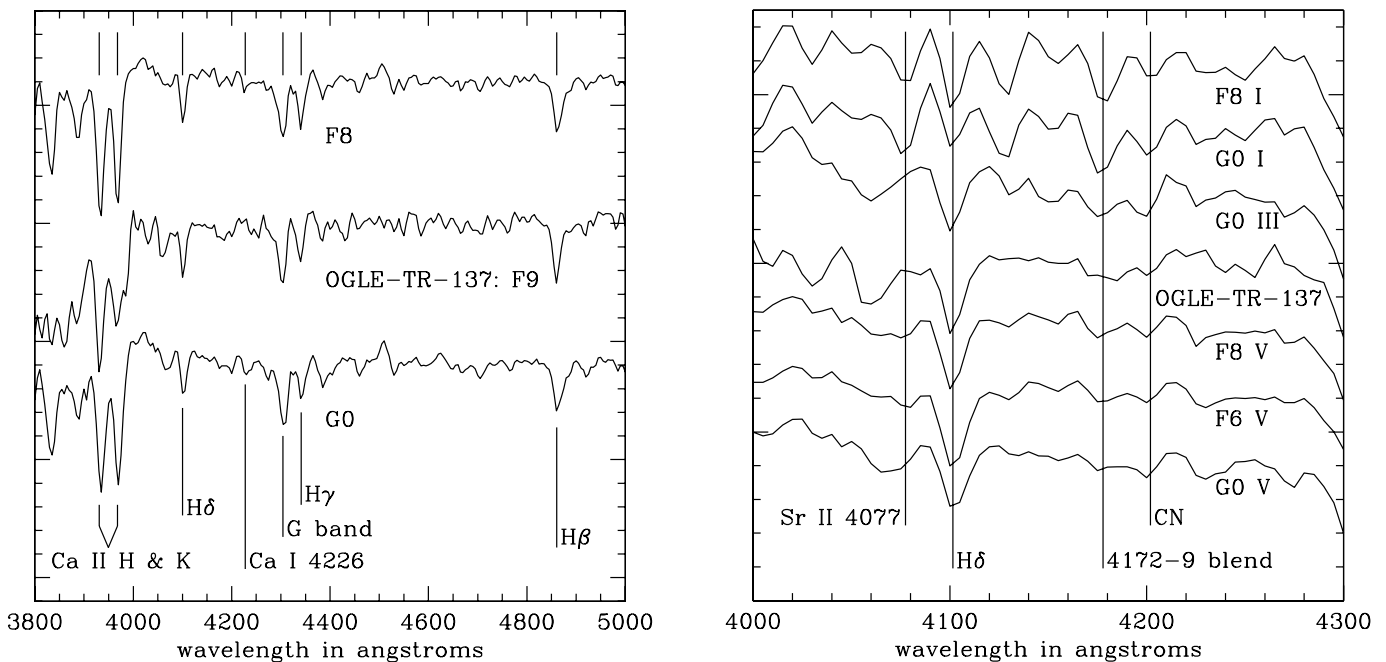


FIG. 4.—Classification of OGLE-TR-137: F9, probable dwarf. The spectral typing is demonstrated on the left and the luminosity classification on the right. The key lines for spectral typing in this regime are the Balmer H lines and the G band, with the intensity of the Balmer lines decreasing and that of the G band increasing toward later spectral types. The lines useful for luminosity classifications are the blend at 4172–4179 Å, the CN feature near 4203 Å, and Sr II  $\lambda$ 4077, which are all stronger in giant stars than in dwarfs. As is clear, spectral type is determined much more confidently than luminosity class. All the comparison spectra are taken from Pickles (1998).

TABLE 2  
SPECTRAL CLASSIFICATION REGIONS

Wavelength Range (Å)	Lines Included	Purpose
3910–4010.....	Ca II H and K	Spectral type
4065–4080.....	Sr II $\lambda$ 4077	Luminosity class
4150–4220.....	CN feature and 4172–4179 Å blend	Luminosity class
4215–4245.....	Ca I $\lambda$ 4226	Spectral type
4260–4320.....	G band	Spectral type
4315–4380.....	H $\gamma$	Spectral type
4810–4910.....	H $\beta$	Spectral type

poor, with larger relative rms errors and occasional egregious misclassifications. Thus, we can expect the science targets to have been classified quite accurately in terms of spectral type, but the luminosities must be considered less confidently. This is especially true when one considers that the signal-to-noise ratio (S/N) of the science target spectra in the vicinity of the luminosity-sensitive lines is quite low, and these lines are shallow. The entire difference, say, in the 4172–4179 Å blend line of an F4 I versus an F4 V may have only a  $2\sigma$  significance on our data from the OGLE stars. By contrast, the S/N of the science targets is not a problem as far as spectral typing is concerned. The lines indicating spectral types are far above the noise level even in our lowest S/N spectrum, that of OGLE-TR-135. This star, like all the others, is confidently classified with an accuracy of 2 spectral subtypes. Figure 2 shows why: H $\gamma$ , the G band, and other temperature-sensitive lines stand out clearly through the noise, and many weaker features shared by the template spectra can also be identified. The confidence with which spectral types can be discerned illustrates why we are not worried by the fact that all four science targets are classified as F types in a sample that would be expected to contain a roughly equal number of F, G, and K stars. The spectral types of our science targets are not biased by noise, and we have already confirmed by classifying stars of known spectral types that our method is

TABLE 4  
SPECTRAL CLASSIFICATIONS OF OGLE STARS

Star	Spectral Type	Luminosity Indication
OGLE-TR-134.....	F2	Probable giant
OGLE-TR-135.....	F6	Probable giant
OGLE-TR-136.....	F8	Probable dwarf
OGLE-TR-137.....	F9	Probable dwarf

NOTES.—The spectral types above are a simple average of the results from the manual and automated classifications. The  $1\sigma$  error of these results is less than 2 spectral subtypes.

not biased toward F stars. The fact that the four targets are all F stars is simply a not-improbable statistical oddity.

Given the above strong caveats about luminosity, can we say anything about the luminosity classes of the science targets at all? Nothing, of course, can be said confidently; however, the good agreement between the automated and manual results for luminosity, and the fact that the automated results for OGLE-TR-136 and 137 are strongly in favor of these stars being dwarfs, suggest that the luminosity results have some meaning. We can say that OGLE-TR-136 and 137 are probably dwarfs, and that OGLE-TR-134 and 135 have a greater likelihood of being giants. We stress, however, that these luminosity classifications are tentative and should not be used to determine plans of future observations. We present our final conclusions on the spectral classifications of the OGLE stars in Table 4.

#### 4. DISCUSSION

The simplest way to interpret our results is to take the spectral types we derive for each star, look up the estimated radii for stars of each type in Cox (2000), and calculate the radii of the transiting object from the depth of the photometric transit. We have accurate spectral types, but we have only tentative and uncertain luminosity classifications, so we cannot confidently determine the radii of our stars. However, if the stars are not dwarfs, it is impossible that the transiting objects could be real planets. Since

TABLE 3  
SPECTRAL CLASSIFICATION RESULTS

Star	Known Classification	Manual Classification	Numerical Auto Type	Numerical Auto Class	Automated Classification
HD 173764.....	G4 IIa	G2 II	25.99	1.34	G6 I
HD 109011.....	K2 V	K3 V	30.27	3.05	K0 III
HD 157999.....	K2 II	K2 II	32.66	2.1	K3 II
HD 126660.....	F7 V	F6 IV	18.35	4.68	F8 V
HD 109358.....	G0 V	G1 V	20.63	4.75	G1 V
HD 164136.....	F2 I	F4 II	12.24	3.03	F2 III
HD 195295.....	F5 II	F3 I	13.58	2.04	F4 II
$\beta$ Leo.....	A3 V	...	1.38	5.00	A1 V
78 UMa.....	F2 V	...	11.16	3.31	F1 III
83 Vir.....	G0 IB	...	22.52	3.66	G3 IV
70 Vir.....	G4 V	...	23.53	4.73	G4 V
61 UMa.....	G8 V	...	28.16	3.68	G8 IV
56 UMa.....	G8 IIB	...	28.3	2.35	G8 II
OGLE-TR-134.....	...	F3 II	11.2	3.29	F1 III
OGLE-TR-135.....	...	F5 II	17	2.9	F7 III
OGLE-TR-136.....	...	F7 V	19.51	4.66	G0 V
OGLE-TR-137.....	...	F8 V	20.16	3.99	G0 IV

NOTES.—“Numerical auto type” refers to the exact numerical value output by the automated classification routine for the spectral type of the star, while “numerical auto class” refers to the exact numerical value for the luminosity class. The “automated classification” column gives the spectral type and luminosity class corresponding to these numerical values, rounded to the nearest integer. It can be seen that the automated classification is more accurate on the spectral type and the manual classification on the luminosity class.

our spectra do not conclusively demonstrate that any one of the stars is not a dwarf, we may calculate the radii of the transiting objects under the assumption that the stars are dwarfs and see whether these radii are small enough that the objects could be planets. If the radius turns out too large, then the transiting object is certainly a star. If not, the companion could be a planet, a brown dwarf, or a very low mass star—or the system could be a blend, as it must certainly be if the star is a giant, as is tentatively indicated by our spectra in some cases.

U03 have published estimated transit depths, but they have not included estimated uncertainties. Since they have kindly made their photometric data available on the World Wide Web,<sup>3</sup> we have performed our own transit fitting and statistical analysis of their data. We have obtained best-fit values and statistical uncertainties for three parameters,  $R_*/a$ ,  $R_T/a$ , and  $R_T/R_*$ , where  $R_*$  is the stellar radius,  $R_T$  is the transiting companion radius, and  $a$  is the orbital separation. In these fits we have assumed a central transit ( $i = 90^\circ$ ), since the photometric data have too much scatter to derive a meaningful value for  $i$ , and a circular orbit, since all extrasolar planets discovered to date with periods as short as these transits have circular or nearly circular orbits (Halbwachs et al. 2005). We have used limb-darkening coefficients for the  $I$  band, in which the U03 observations were made, appropriate for a star of spectral type approximately F5 ( $\log g = 4.5$ ;  $T_{\text{eff}} = 6750$  K). We obtained these from the tables described in Van Hamme (1993).<sup>4</sup> Changes in the fit parameters due to differences in limb-darkening between an F2 star and an F9 star are expected to be negligible. If the assumption of a central transit is violated, significantly different larger values for  $R_*/a$  and  $R_T/a$  will apply. The reason for this is that in the transit fit the length of the photometric transit determines the fit value of  $R_*/a$ , and the fit value of  $R_*/a$  combined with the depth of the photometric transit determines  $R_T/a$ . If the transit is noncentral, the fit performed under the central transit assumption will incorrectly interpret the transit length as a measure of the full diameter of the star, when in reality it measures the shorter chord the companion traverses across the face of the star. Thus, the fit radius of the star will be smaller than its true radius, and because of this the radius of the transiting companion will also be underestimated. The fit value of  $R_T/R_*$  is less sensitive to violation of the central transit assumption, but it is still to some extent an underestimate if the assumption is violated, because the companion then traverses more limb-darkened regions of the stellar disk and must be slightly larger to cause the same transit depth. All three fit parameters are to be regarded as lower limits, but since grazing transits are statistically rare, it is likely that the true values, in particular the ratio  $R_T/R_*$ , lie near the fits.

In Table 5 we present the results of our transit fits, and in Table 6 we show the lower limit radii we deduce for the transiting companions. It remains to be asked, what is the maximum radius for a planet? The best measurement to date of the radius of an extrasolar planet is that of Brown et al. (2001), who measured the radius of HD 209458b at  $1.347 \pm 0.060 R_J$  using photometry from the *Hubble Space Telescope* STIS. Burrows et al. (2003) show that theoretical models of HD 209458b tend to favor a radius at the low end of the Brown et al. (2001) error bar. The mass of HD 209458b is  $0.69 \pm 0.05 M_J$  (Brown et al. 2001), which is well below the maximum mass for a planet. However, more massive planets are not expected to be larger in radius, at least up to  $3 M_J$

TABLE 5  
RESULTS OF FITTING U03 TRANSIT DATA

Star	$R_T/a$	$R_*/a$	$R_T/R_*$
OGLE-TR-134 .....	$0.0089^{+0.0008}_{-0.0010}$	$0.0921^{+0.0067}_{-0.0112}$	$0.0963 \pm 0.0061$
OGLE-TR-135 .....	$0.0264 \pm 0.0016$	$0.2271^{+0.0090}_{-0.0089}$	$0.1164 \pm 0.0066$
OGLE-TR-136 .....	$0.0141^{+0.0020}_{-0.0013}$	$0.1349^{+0.0221}_{-0.0087}$	$0.1046 \pm 0.0087$
OGLE-TR-137 .....	$0.0192 \pm 0.0014$	$0.1303^{+0.0067}_{-0.0068}$	$0.1470 \pm 0.0104$

NOTES.—Asymmetrical  $2\sigma$  uncertainties are quoted for  $R_*/a$  and  $R_T/a$ . For  $R_T/R_*$  we quote approximate symmetrical  $2\sigma$  uncertainties. Our fit implies that for  $R_T/R_*$ , unlike  $R_*/a$  and  $R_T/a$ , symmetrical uncertainties are always a good approximation.

(Bodenheimer et al. 2003). Thus, we conclude that HD 209458b is near the maximum radius for an extrasolar planet, and we adopt  $1.4 R_J$  as the radius above which we conclude that an object is not a planet and is probably a low-mass star. Bringing this number to Table 6, we find that OGLE-TR-137 is completely eliminated as a transiting planet candidate, but the others are statistically consistent with being planets. OGLE-TR-134 and 136 in particular appear to be good candidates based on this analysis.

There is one additional test that is possible with the data that have been obtained so far. U03 estimate the radii (and masses) of the stars and the radii of their companions based on the transit data alone, with no spectroscopic information. Although U03 do not explain exactly how their masses and radii are derived, the basic principle is clear. The period of the transit provides, via Kepler's law, an equation connecting the mass of the star  $M_*$  to the semimajor axis  $a$  of the companion's orbit:

$$a = \frac{P^{2/3} M_*^{1/3} G^{1/3}}{(2\pi)^{2/3}}, \quad (1)$$

where  $P$  is the period of the transiting companion, published by U03. The ratio of the transit length to the orbital period can be simply related to the ratio of  $R_*$  to  $a$ :

$$\alpha = \frac{R_* \gamma}{\pi a}, \quad (2)$$

where  $\alpha$  is the ratio of the transit length to the orbital period  $P$ , and  $\gamma \leq 1.0$  is a factor to include the possibility of a noncentral transit; that is, it is the ratio of the length of the chord the companion actually traverses across the star to the diameter of the star. Finally, a mass-radius relation for main-sequence stars provides the third equation needed to solve for the three unknowns  $M_*$ ,  $R_*$ , and  $a$ , under the assumption that the transit is central and the primary is a main-sequence star. U03 use the mass-radius relation:

$$\frac{R_*}{R_\odot} = \left( \frac{M_*}{M_\odot} \right)^{4/5}. \quad (3)$$

This can be combined with equations (1) and (2) to give a solution for the mass:

$$\frac{M_*}{M_\odot} = \frac{\pi^{15/7} \alpha^{15/7} P^{10/7} G^{5/7} M_\odot^{5/7}}{(2\pi)^{10/7} \gamma^{15/7} R_\odot^{15/7}}, \quad (4)$$

from which, of course, a solution for the radius follows trivially. Our statistical analysis of the U03 photometry gives the value of  $R_*/a = \pi\alpha$  directly, under the assumption of a central transit ( $\gamma = 1.0$ ). If the transit is not central, the value returned by our

<sup>3</sup> At [ftp://ftp.astroww.edu.pl/ogle/ogle3/transits/new\\_2001\\_2002/phot](ftp://ftp.astroww.edu.pl/ogle/ogle3/transits/new_2001_2002/phot).

<sup>4</sup> These limb-darkening tables can be found at <http://www.fiu.edu/~vanhamme/limdark.htm>.

TABLE 6  
RADII OF TRANSITING OBJECTS

Star	Spectral Type	$R_T/R_*$	Star Radius ( $R_\odot$ )	Companion Radius ( $R_J$ )
OGLE-TR-134 .....	F2	$0.0963 \pm 0.0061$	$1.42 \pm 0.08$	$1.33 \pm 0.11$
OGLE-TR-135 .....	F6	$0.1164 \pm 0.0066$	$1.26 \pm 0.08$	$1.43 \pm 0.12$
OGLE-TR-136 .....	F8	$0.1046 \pm 0.0087$	$1.18 \pm 0.08$	$1.20 \pm 0.13$
OGLE-TR-137 .....	F9	$0.1470 \pm 0.0104$	$1.14 \pm 0.08$	$1.63 \pm 0.16$

NOTES.—The stellar radii are from our spectral types and the tabulated radii in Cox (2000), assuming all the stars are dwarfs. The uncertainties in the stellar radii assume a classification uncertainty of  $\pm 2$  subtypes. The ratio of transiting companion radius to stellar radius,  $R_T/R_*$ , is from our statistical fits to the U03 photometry, and we quote approximate  $2 \sigma$  uncertainties.

analysis as  $R_*/a$  will be approximately equal to  $R_*\gamma/a$ , which is equal to  $\pi\alpha$  regardless of whether  $\gamma = 1.0$ . Thus, we use a slightly different form of equation (4):

$$\frac{M_*}{M_\odot} = \frac{(R_*\gamma/a)^{15/7} P^{10/7} G^{5/7} M_\odot^{5/7}}{(2\pi)^{10/7} \gamma^{15/7} R_\odot^{15/7}}. \quad (5)$$

We use the results of our statistical analysis of the U03 photometry in equation (5) to obtain values for  $M_*$  and  $R_*$  based on the U03 photometric transit alone. The usefulness of this is that inconsistency between the lower limit on  $R_*$  obtained from the photometry and the value of  $R_*$  inferred from the spectral type can indicate that the assumption that the star is a main-sequence object is incorrect, in which case, of course, it is no longer a planetary transit candidate. We present the results obtained from equation (5) alongside the radii inferred from our spectra in Table 7. Examination of Table 7 shows that there are serious discrepancies between the values derived from fitting the U03 transit light curves and those we infer from our spectral types under the assumption that the stars are unblended dwarfs.

In the case of OGLE-TR-134 and 137 the discrepancy is in the sense we would expect: the spectroscopic radii and masses are larger than the photometric lower limits. This, of course, is not a true discrepancy at all; it simply implies that the assumption  $\gamma = 1.0$  is violated. The implied values for  $\gamma$  are  $0.874^{+0.069}_{-0.109}$  for OGLE-TR-134 and  $0.968^{+0.071}_{-0.072}$  for OGLE-TR-137, where uncertainties in both the value of  $R_*\gamma/a$  derived from photometry and in the parameters inferred from the spectral types have been taken into account. Values of  $\gamma$  greater than 1.0, statistically permitted in the case of OGLE-TR-137, do not, of course, correspond to any physically possible situation. The values of the inclination  $i$  corresponding to the allowed range of  $\gamma$  are  $87^\circ 07'_{-1221}^{+0778}$  for OGLE-TR-134 and  $88^\circ 07'_{-222}^{+220}$  for OGLE-TR-137. Once again,

values of  $i$  greater than  $90^\circ 0$  do not correspond to any physical reality; error bars extending above  $90^\circ 0$  are simply an indication that  $i = 90^\circ 0$  is statistically permitted. Note that  $i = 90^\circ 0$  is permitted for OGLE-TR-137 but not for OGLE-TR-134. In neither case are grazing or near-grazing transits, in which the outer limb of the planet is outside or just inside the limb of the star at midtransit, permitted. This is fortunate, because it indicates that the inclinations of these two systems lie in the regime in which the approximations we have made in the above analysis are good. In particular, the values of  $R_T/R_*$  are accurate, provided the systems are not blends.

We note as a caveat to the above that although U03 detected seven transits for OGLE-TR-137, allowing them to confidently determine its period, they detected only two for OGLE-TR-134, which means that their value for its period may be incorrect by a factor that is a small integer or a ratio of small integers. The error would be in the sense that the true period is longer than the one they report, since it is their practice to choose the shortest period consistent with the data when there is ambiguity (Udalski et al. 2002c). If the period were increased, the ratio of transit duration to orbital period,  $\alpha$  in equation (4), would, of course, decrease by the same factor as, necessarily, would the value  $R_*\gamma/a = \pi\alpha$  output by our fits to the U03 photometry and used in equation (5). Since the power of  $\alpha$  or  $R_*\gamma/a$  is greater than that of  $P$  in equations (4) and (5), the net effect would be that the calculated stellar mass would decrease. The result could still be brought into agreement with the mass implied by the spectral type by hypothesizing a lower value for  $\gamma$ . This value would likely still be reasonable, as  $\gamma$  would vary only as the  $-1/3$  power of  $P$ , but if  $P$  were very much larger than the U03 value, a grazing transit might be implied.

In the case of OGLE-TR-136 the radius and mass obtained from our spectral types lie below the lower limits from our fit to the photometric light curve. The basic reason for the problem

TABLE 7  
STELLAR MASSES AND RADII FROM PHOTOMETRY

Star	$P$ (days)	$R_*\gamma/a$	$M_{\text{phot}}$ ( $M_\odot$ )	$M_{\text{spec}}$ ( $M_\odot$ )	$R_{\text{phot}}$ ( $R_\odot$ )	$R_{\text{spec}}$ ( $R_\odot$ )
OGLE-TR-134 .....	4.5372	$0.0921^{+0.0067}_{-0.0112}$	$1.14^{+0.19}_{-0.28}$	$1.52 \pm 0.08$	$1.11^{+0.14}_{-0.22}$	$1.42 \pm 0.08$
OGLE-TR-135 .....	2.5733	$0.2271^{+0.0090}_{-0.0089}$	$3.50^{+0.30}_{-0.29}$	$1.33 \pm 0.12$	$2.73^{+0.19}_{-0.18}$	$1.26 \pm 0.08$
OGLE-TR-136 .....	3.1158	$0.1349^{+0.0221}_{-0.0087}$	$1.51^{+0.58}_{-0.20}$	$1.19 \pm 0.14$	$1.39^{+0.41}_{-0.15}$	$1.18 \pm 0.08$
OGLE-TR-137 .....	2.53782	$0.1303^{+0.0067}_{-0.0068}$	$1.045^{+0.12}_{-0.11}$	$1.12 \pm 0.12$	$1.04 \pm 0.09$	$1.14 \pm 0.08$

NOTES.—The periods are from U03, and the values for  $R_*\gamma/a$  are those returned as  $R_*/a$  by our statistical analysis of the U03 photometry with  $\gamma$  assumed to be 1.0; we quote asymmetrical  $2 \sigma$  error bars. The values for  $M_{\text{phot}}$  and  $R_{\text{phot}}$  are obtained from the period and  $R_*\gamma/a$  using eq. (5), and once again asymmetrical  $2 \sigma$  error bars are quoted. The values are lower limits because we have set  $\gamma$  to 1.0 in eq. (5). The  $M_{\text{spec}}$  and  $R_{\text{spec}}$  values are based on our spectral types and interpolated from the tables in Cox (2000) under the assumption that the stars are dwarfs.

is that the transit is longer relative to the period (thus  $\alpha$ , or equivalently  $R_*\gamma/a$ , is larger) than one expects for a main-sequence star within 2 spectral subtypes of F6. This problem cannot, of course, be resolved by hypothesizing  $\gamma < 1.0$ . The uncertainties almost, but not quite, permit a statistical resolution. If we calculate a value for  $\gamma$  in the same manner as for OGLE-TR-134 and 137 we obtain  $\gamma = 1.117^{+0.195}_{-0.099}$ . Unfortunately, nothing in the statistically permitted range corresponds to a physically possible situation. The nearest physically possible point,  $\gamma = 1.0$ , lies just outside the error bars.

The discrepancy is much worse for OGLE-TR-135. The radius and mass inferred from spectroscopy in its case are far below the lower limits obtained from the photometric light curve. Calculation of  $\gamma$  leads to an entirely meaningless result,  $\gamma = 1.571^{+0.099}_{-0.098}$ , which deviates from the highest physically permissible value,  $\gamma = 1.0$ , by almost 6 times the lower error bar.

What do the discrepancies between spectroscopic and photometric masses and radii tell us about OGLE-TR-135 and 136? They may indicate that the stars are blends. If this is true, the F star that we observed in our spectra, which may be either a giant or a dwarf, is unresolvably combined with a fainter eclipsing binary that is probably a physically unrelated background or foreground object. The relatively deep eclipses of the binary, diluted by the brighter F star, cause the shallow, transit-like signal. Since the U03 light curves do not show a detectable secondary eclipse, the binary has either a high mass ratio so that secondary eclipses are undetectable or a mass ratio near 1.0 so that secondary and primary eclipses are indistinguishable. If the mass ratio is high, equations (1)–(5) still apply, but to the eclipsing binary, not to the star that dominates the spectrum. Of course, the true eclipse depth is then unknown, but it is certainly much deeper than the measured transit depth, and the eclipsing object is a star.

Are explanations other than blends possible? The derivations of equations (4) and (5) assume that the mass of the transiting companion is small compared to the mass of the star. If it is not, the equations must be altered. However, the alteration changes the solutions in the same sense as hypothesizing  $\gamma$  less than 1.0, i.e., in the wrong direction to remove the discrepancy for OGLE-TR-135 and 136. What about the possibility that OGLE-TR-135 and 136 are unblended stars that for some reason do not follow the mass-radius relation equation (3) or do not have the masses and radii we assigned them from their spectral types using the tables in Cox (2000)? Certainly, real stars show some scatter about equation (3). Indeed, the masses and radii of the Cox (2000) tables themselves do not exactly follow this relation. Likewise, of course, not all F6 or F8 stars can be expected to have radii exactly equal to the values we have obtained for them from interpolation of the Cox (2000) tables. Hypothesizing that the reason for the discrepancy is that the primary simply has an abnormal mass and radius for its spectral type and/or does not lie exactly along the equation (3) curve seems reasonable in the case of OGLE-TR-136 because the discrepancy is so small. We consider this a definite possibility. While we do not feel that a similar scenario for OGLE-TR-135 can be completely ruled out, it does seem much less likely because the discrepancy is so large. In order to explain the observed value of  $R_*\gamma/a$ , or equivalently  $\alpha$ , the star would be required to have a density significantly less than that of a typical main-sequence F6 star (otherwise  $\alpha$  would be lower than observed) but far higher than that of a giant (otherwise  $\alpha$  would be far higher than observed). If the star has such an intermediate density, high-resolution spectroscopy will reveal a surface gravity lower than expected for dwarfs but still much higher than that of giants. However,

stars with such intermediate properties are probably quite short-lived objects that have just left the main sequence and are in transit to the giant branch. We would expect them to be rare.

There is a final test that is possible with additional archival data. Gallardo et al. (2005) make use of near-IR data, both from the Two Micron All Sky Survey (2MASS) and from observations of their own, in their analysis of OGLE transiting candidates from Udalski et al. (2002b). We have not carried out near-IR observations of OGLE-TR-134 through 137, but data from 2MASS may still be useful. Duplicating in full the sophisticated analysis of Gallardo et al. (2005) is beyond the scope of this work and is not warranted by the uncertain nature of 2MASS counterparts in the very crowded Galactic bulge fields in which our stars are found. Two of our stars do have apparent 2MASS counterparts, however, and we would be remiss not to obtain the key piece of information the 2MASS data can provide us: a measure of the interstellar extinction to the two stars. We cannot measure the extinction directly from our spectra because, due to the necessarily high air mass at which we did the observations, we do not have a spectrophotometric calibration.

We find possible 2MASS counterparts for OGLE-TR-135 and 136. We do not find a counterpart for OGLE-TR-134 because 2MASS does not resolve it from a nearby star of similar *I*-band brightness that is visible on the U03 finder chart. OGLE-TR-137 is simply too faint for 2MASS to detect. Our possible 2MASS counterpart for OGLE-TR-135 lies about 1".1 from the U03 coordinates, at a position angle of about 184°. The 2MASS astrometric uncertainties listed for this object are about 0".2, and U03 do not quote position uncertainties. The U03 chart for OGLE-TR-135 shows that there is a star significantly dimmer in the *I* band approximately 1".4 away from OGLE-TR-135 at roughly position angle 210°. Thus, the location of the 2MASS object appears to be statistically inconsistent with OGLE-TR-135 but consistent with the dimmer nearby star shown on the U03 chart. It is possible that this star could be brighter than OGLE-TR-135 in the near-IR, so that 2MASS detected it and not OGLE-TR-135. It also seems possible, however, that the 2MASS object is OGLE-TR-135 and that the positional discrepancy simply results from a small error in either the 2MASS or the U03 position. We proceed to consider the 2MASS object to be a detection of OGLE-TR-135, with a warning to the reader to remember that it may instead be the dimmer companion shown on the U03 chart. For OGLE-TR-136 the U03 chart shows no stars of comparable brightness within a few arcseconds, and there is a 2MASS counterpart that matches the U03 position to within the 2MASS astrometric uncertainties.

The 2MASS sources associated with OGLE-TR-135 and 136 are detected in the 2MASS *H*-band observations but not in *J* or *K<sub>s</sub>*. Both are listed as detections with S/N greater than 5 but less than 7, with a flag warning that confusion from nearby brighter stars may have affected the measurements. Using *H* magnitudes from 2MASS, *I* magnitudes from U03, and *I* – *H* values for dwarf stars interpolated from tables in Cox (2000), we find an *I* – *H* reddening of  $1.226 \pm 0.185$  for OGLE-TR-135 and  $0.369 \pm 0.123$  for OGLE-TR-136, where the uncertainties include 2MASS errors only. From Sumi (2004) we find that the extinction ratio  $A(I)/A(V)$  is typically about 0.49 in the OGLE bulge fields. Cox (2000) has  $A(I)/A(V) = 0.479$  for  $R_V = 3.1$ , so we conclude that the other Cox (2000) extinction ratios for  $R_V = 3.1$  are applicable to the extinction in the direction of our stars. From these, we obtain  $A(I)/A(H) = 2.722$ , and thus  $A(I) = 1.94 \pm 0.29$  for OGLE-TR-135 and  $A(I) = 0.58 \pm 0.19$  for OGLE-TR-136. The Sumi (2004) map shows that the extinctions to the galactic bulge in the directions of these two stars

are about  $A(I) = 1.813$  and  $A(I) = 1.47$ , respectively. This suggests that OGLE-TR-135 is at or near the distance of the galactic bulge, but OGLE-TR-136 is located well short of the bulge. If OGLE-TR-135 is located at 8 kpc, the approximate distance to the galactic bulge, and is extinguished by 1.813 mag in the  $I$  band, its absolute  $I$  magnitude is  $-1.17$ . By contrast, from Cox (2000) we have that the absolute  $I$  magnitude of an F6 V star is 2.99. It appears, therefore, that if the 2MASS counterpart does represent an accurate measurement of the  $H$ -band brightness of OGLE-TR-135, the star is a bulge giant. OGLE-TR-136, however, appears to lie well short of the bulge. If it is a normal F8 V star, with an absolute  $I$  magnitude of 3.24 as obtained from Cox (2000), the implied distance is 1.67 kpc, or about 20% of the way to the bulge. The extinction we calculate for this star is nearly 40% of the bulge extinction, which seems at odds with the star being at only 20% of the bulge distance; however, because of the patchiness of galactic extinction, the scenario seems possible.

## 5. CONCLUSIONS

The star OGLE-TR-134, if an unblended dwarf, is orbited by an object of planetary dimensions. This object could be a planet, a brown dwarf, or a very low mass star. Which of these it is can be determined by precision radial velocity monitoring to determine its mass. Our luminosity classification tentatively indicates that OGLE-TR-134 could be a giant. If this were the case, the system would be an F giant blended with a fainter eclipsing binary and, of course, would not contain a planet. We place very little confidence in our luminosity classifications, however, and no other evidence suggests that OGLE-TR-134 is a blend. We therefore consider it to be retained as a good planetary transit candidate. It is probably the best of the four candidates we have investigated.

OGLE-TR-135 does not represent a system containing a transiting planet. If the star is an unblended dwarf, it is orbited by an object that may be small enough to be a planet. However, the large discrepancy between the stellar parameters determined from the U03 transit fitting and those we infer from our spectra provides strong evidence that the star is a blend. Furthermore, both our spectra and our analysis of 2MASS data suggest the star is a bulge giant. While neither of these lines of evidence is strong in itself, they combine with the discrepancy between spectral and photometric parameters to provide a strong case that the star we identify in our spectra is a giant located in the bulge. It is very likely that the object is a blend of an F star with a fainter eclipsing binary. It is unlikely but possible that the object is an unblended transiting system with an anomalous primary star, but even in this case the observed transit depth and the anomalously large radius of the primary will require the companion to have stellar dimensions. A planetary interpretation is confidently excluded.

If the star OGLE-TR-136 is an unblended dwarf, it is orbited by an object of planetary size whose true nature could be determined by precision radial velocity measurements revealing its mass. As in the case of OGLE-TR-135, a discrepancy exists between the stellar parameters obtained from transit fitting and those from our spectral type. While this may indicate that the system is a blend, the discrepancy is far less than that for OGLE-TR-135 and thus does not demand such an interpretation. The star may simply have a slightly anomalous radius and mass for its spectral type. We note that the inferred companion radius for OGLE-TR-136 is only  $1.20 \pm 0.13 R_J$ , the lowest among the four stars we have studied and sufficiently well within the allowed range for planets that the transiting object could still have planetary dimensions even if the primary is an anomalous main-sequence star with a larger radius than we have inferred from our

spectra. We thus retain OGLE-TR-136 as a good planetary transit candidate.

The star OGLE-TR-137, if an unblended dwarf, is orbited by an object with the dimensions of a low-mass star. The system does not contain a transiting planet. However, there is no evidence that the system is a blend, and U03 were able to confidently determine the period. The result is that of the four systems we have investigated, OGLE-TR-137 is the one whose nature can be most confidently identified. It is very likely an eclipsing binary consisting of a dwarf with spectral type near F9 orbited by a low-mass star with radius near  $1.6 R_J$  and thus spectral type later than M6 and mass below  $0.12 M_\odot$ . As such, it is interesting in its own right, because further photometry and radial velocity monitoring could accurately determine the mass and radius of the companion, which would provide useful constraints on theoretical models of low-mass stars.

## 6. RECOMMENDED FUTURE OBSERVATIONS

Assuming that the U03 period for OGLE-TR-134 is correct, it is a good planetary transit candidate and should certainly be observed with high-resolution spectroscopy for precise radial velocity monitoring. However, the period may be uncertain. At least one transit should be observed photometrically to confirm and refine the period measurement. Such an observation might also be important to obtain improved phase information needed to interpret the radial velocity observations, since most of the OGLE photometry of OGLE-TR-134 is from 2001 and the phase has thus probably become somewhat uncertain.

OGLE-TR-135 does not appear to be a good candidate for further observations. We are confident that it is not a transiting planetary system.

Although there is a slight discrepancy between the stellar parameters derived from spectra and from transit fitting for OGLE-TR-136, it remains a good planetary transit candidate that should be subjected to high-precision radial velocity monitoring. The high-resolution spectra required for such monitoring should also be analyzed to obtain  $\log g$  of the star and determine if it is indeed a main-sequence object with a slightly larger radius and lower density than a normal F8 V star, as we suggested above.

OGLE-TR-137 is conclusively ruled out as a planetary system based on the large radius for the companion that is implied by our result for the primary's spectral type. The system is probably a high mass ratio eclipsing binary with a main-sequence primary of spectral type near F9 orbited by a low-mass secondary. As such, it may be an interesting system in its own right because of its potential to constrain theoretical models of low-mass stars. It should be subjected to further photometry to measure the radii of the two stars and to radial velocity monitoring to measure their masses. This radial velocity monitoring need not have sufficient sensitivity to detect a planet.

This research has made use of the SIMBAD database, operated at CDS, Strasbourg, France. This publication makes use of data products from the Two Micron All Sky Survey, which is a joint project of the University of Massachusetts and the Infrared Processing and Analysis Center, California Institute of Technology, funded by the National Aeronautics and Space Administration and the National Science Foundation. This research has made extensive use of information and code from Press et al. (1992).

## REFERENCES

- Abt, H. A., Meinel, A. B., Morgan, W. W., & Tapscott, I. W. 1968, *An Atlas of Low-Dispersion Grating Stellar Spectra* (Tucson: Kitt Peak Natl. Obs.)
- Bodenheimer, P., Laughlin, G., & Lin, D. N. C. 2003, *ApJ*, 592, 555
- Bouchy, F., Pont, F., Santos, N. C., Melo, C., Mayor, M., Queloz, D., & Udry, S. 2004, *A&A*, 421, L13
- Brown, T. M., Charbonneau, D., Gilliland, R. L., Noyes, R. W., & Burrows, A. 2001, *ApJ*, 552, 699
- Burrows, A., Sudarsky, D., & Hubbard, W. B. 2003, *ApJ*, 594, 545
- Cox, A. N. 2000, *Allen's Astrophysical Quantities* (4th ed.; New York: Springer)
- Dreizler, S., Rauch, T., Hauschildt, P., Schuh, S. L., Kley, W., & Werner, K. 2002, *A&A*, 391, L17
- Gallardo, J., Minniti, D., Valls-Gabaud, D., & Rejkuba, M. 2005, *A&A*, 431, 707
- Halbwachs, J. L., Mayor, M., & Udry, S. 2005, *A&A*, 431, 1129
- Konacki, M., Torres, G., Sasselov, D. D., & Jha, S. 2003, *ApJ*, 597, 1076
- Pickles, A. J. 1998, *PASP*, 110, 863
- Pont, F., Bouchy, F., Queloz, D., Santos, N. C., Melo, C., Mayor, M., & Udry, S. 2004, *A&A*, 426, L15
- Press, W. H., Teukolsky, S. A., Vetterling, W. T., & Flannery, B. P. 1992, *Numerical Recipes in C* (2nd ed.; New York: Cambridge Univ. Press)
- Silva, D. R., & Cornell, M. E. 1992, *ApJS*, 81, 865
- Sirko, E., & Paczynski, B. 2003, *ApJ*, 592, 1217
- Sumi, T. 2004, *MNRAS*, 349, 193
- Udalski, A., Pietrzynski, G., Szymanski, M., Kubiak, M., Zebrun, K., Soszynski, I., Szewczyk, O., & Wyrzykowski, L. 2003, *Acta Astron.*, 53, 133 (U03)
- Udalski, A., Szewczyk, O., Zebrun, K., Pietrzynski, G., Szymanski, M., Kubiak, M., Soszynski, I., & Wyrzykowski, L. 2002a, *Acta Astron.*, 52, 317
- Udalski, A., Zebrun, K., Szymanski, M., Kubiak, M., Soszynski, I., Szewczyk, O., Wyrzykowski, L., & Pietrzynski, G. 2002b, *Acta Astron.*, 52, 115
- Udalski, A., et al. 2002c, *Acta Astron.*, 52, 1
- van Dokkum, P. G. 2001, *PASP*, 113, 1420
- Van Hamme, W. 1993, *AJ*, 106, 2096